 doi:10.20944/preprints202010.0328.v1

Article

Correlating grip force signals from multiple sensors highlights functional synergies of manual control in a complex task-user system

Birgitta Dresp-Langley [1]*, Florent Nageotte [2], Philippe Zanne [2] and Michel de Mathelin [2]

[1] ICube UMR 7357 Centre National de la Recherche Scientifique (CNRS) 1; birgitta.dresp@unistra.fr;
[2] ICube UMR 7357 Robotics Department University of Strasbourg; nageotte@unistra.fr; philippe.zanne@unistra.fr; demathelin@unistra.fr;
* Correspondence: birgitta.dresp@unistra.fr;

Abstract: Biosensors and wearable sensor systems with transmitting capabilities are currently developed and used for the monitoring of health data, exercise activities, and other performance data. Unlike conventional approaches, these devices enable convenient, continuous, and unobtrusive monitoring of a user's behavioral signals in real time. Examples include signals relative to hand an finger movement/pressure control reflected by individual grip force data. As will be shown here, these directly translate into task, skill and hand-specific (dominant *versus* non-dominant hand) grip force profiles for different measurement loci in the fingers and palm of the hand. On the basis of thousands of sensor data from multiple sensor locations, individual grip force profiles of an task expert, a trained user and a highly proficient user (expert) performing an image-guided and robot-assisted precision task with the dominant or the non-dominant hand are analyzed in several steps following Tukey's "detective work" approach. Correlation analyses (Person's Product Moment) reveal skill-specific differences in individual grip force profiles across multiple sources of variation, functionally mapped to the somatosensory brain networks which ensure grip force control and its evolution with control expertise. Implications for the real-time monitoring of individual grip force profiles and their evolution with training in complex task-user systems are brought forward.

Keywords: wearable biosensors; wireless technology; human grip force; motor control; complex task-user systems; expertise; multivariate data; correlation analysis; functional analysis

1. Introduction

The Biosensors and wearable sensor systems with transmitting capabilities represent innovative technology developed to monitor exercise and other task activities [1]. Unlike conventional approaches, these new devices enable convenient, continuous, and/or unobtrusive monitoring of a user's behavioral signals in real time, including signals relative to individual grip forces, recorded from multiple sensor locations on the user's hands. Wearable sensor systems combine innovation in sensor design, electronics, data transmission, power management, and signal processing for the statistical analysis of thousands of data recorded from multiple locations (*big data*). Many technological aspects still remain to be optimized. To read meaning into such a multitude of signal variations, functionally driven methods of analysis and visualization are needed, as will be shown here on the example of step-by-step statistical "detective work". John W. Tukey [2] was among the first to explicitly compare the analysis of complex data to "good detective work". Such should not be fully automated, but may benefit from wisely and adequately developed automated steps within a functionally driven strategy. Good detective work in multivariate data analysis has to start by asking the right question(s), then look for the right clues and, finally, draw the right conclusions from the clues available. This is illustrated here on the basis of thousands of grip force signals recorded from multiple locations in the dominant and dominant hands of users

 doi:10.20944/preprints202010.0328.v1

with varying levels of expertise in the manual control of a robotic task device. In particular, it is shown how functionally meaningful signal correlations are obtained from such a multitude of spatiotemporally variable grip force profiles. Human grip force is controlled at several hierarchical stages, from sensory receptors to the brain and back to the hand, and its functional aspects have been relatively well studied. For example, the relationship between individual finger positions and grip forces of men and women, when subjects hold cylindrical objects from above, using circular precision grips in the 5-finger grip mode, revealed effects of 4-, 3- and 2-finger grip modes [3]. Individual finger position was nearly constant for all weights and for diameters of 5.0 and 7.5 cm. There were no differences in individual finger position with regard to gender, hand dimension, or hand strength. Total grip force also increased as the number of fingers used for grasping decreased. In the contribution of the individual fingers to the total grip force, the thumb's contribution is followed by that of the ring finger and the little finger (pinky), which contributes approximately 18-23% for all weights and object diameters tested. The contribution of the index finger is always the smallest, and there is no gender difference for any of the grip force variables tested [3]. Effects of hand dimension and hand strength on the individual finger grip forces are generally subtle and minor. Contribution and co-ordination of finger grip forces in precision grip tasks using multiple fingers is reflected by large changes in finger force recorded from the index finger, followed by the middle, ring, and little fingers [4]. Results suggest that all individual finger force adjustments for lighter loads (<800 g) are controlled by a single common scaling value, and the fewer the number of fingers used, the greater the total grip force [4]. The grip mode, i.e. whether all five or only three fingers are used, influences the force contributions of the middle and ring fingers, but not that of the index finger [4]. Other studies have shown a phenomenon of motor redundancy in human prehensile behavior [5]. The partly redundant design of the hand allows performing a variety of tasks in a reliable and flexible way following the principle of abundance, as shown in robotics with respect to the control of artificial grippers, for example. Multi-digit synergies appear to operate at two levels of hierarchy to control prehensile action [5]. Forces produced by the thumb and the "virtual finger" (an imagined finger with a mechanical action equal to the combined mechanical action of all other four fingers of the hand) co-vary at a higher level only to stabilize the grip action in respect to the orientation of the hand-held object. Analysis of grip force adjustments during motion of hand-held objects suggests that the central nervous system adjusts to gravitational and inertial loads differently, at an even higher level of control. Object manipulation by efficient control of finger and grip force is therefore not only a motor skill but also a highly cognitive skill [6] that requires multisensory integration and is exploited in surgery, craft making, and musical performance. Sequences of relatively straightforward cause-effect links directly related to mechanical constraints lead on to a non-trivial co-variation between low-level and high-level control variables [4,5,6], as in playing a musical instrument, which requires independent control of the magnitude and rate of force production, which typically vary in relation to loudness and tempo [6]. The expert performance of a highly skilled pianist, for example, is characterized by a rapid reduction of finger forces, allowing for considerably fast performance of repetitive piano keystrokes [6]. Skilled grasping behavior (multi-finger grasping) has three essential components: 1) manipulation force, or resultant force and moment of force exerted on the object and the digits' contribution to force production, 2) internal forces, which are defined as forces that cancel each other out to maintain object stability, to ensure slip prevention, tilt prevention, and robustness against perturbation, and 3) motor control (or grasp control), which involves prehensile synergies, chain effects, inter-finger connection [3,4,5] and the high-level brain command of simultaneous digit adjustments to several, mutually reinforcing or conflicting demands. Prehensile synergies are reflected by the characteristics of single digit action as well as by their their co-variation patterns during task execution [7,8]. Sharing of force patterns across the digits minimizes mechanically unnecessary digit forces, resulting in a trade-off between multi-digit synergies at the two levels of control hierarchy mentioned here above [9]. Grip force using all five fingers may be, depending on the task, equivalent to grip strength without the thumb. The force contributions of the index and the middle finger are generally the most important [10], followed by combinations of the ring and little finger (pinky). The

Preprints (www.preprints.org) | NOT PEER-REVIEWED | Posted: 15 October 2020 doi:10.20944/preprints202010.0328.v1

dominant hand in general generates smaller force contributions of the thumb and the ring finger, and greater force contributions of the palm of the hand [10]. Left handers are less consistent compared to right handers in performing better with their dominant hands [11]. It is currently suggested that the right and left brain hemispheres may each represent the movements of the contralateral, not the ipsilateral hand, however, the programming of isometric fingertip forces is initially based on internal memory representations of physical device properties in addition to visual and haptic information from the current manipulations. These central memory representations are not necessarily lateralized [12-16], and permit anticipatory control of forces, scaled in advance, as explained here above. This allows for a quick and accurate adjustment of grip forces well beyond limitations due to lateralization of internal representation, or a sole dependency on ongoing sensory feedback. Functionally specific neural networks for grip force representation and control relate to the somatosensory cortical network [16], or S1 map, in the primate brain. S1 refers to a neocortical area that responds primarily to tactile stimulations on the skin or hair. Somatosensory neurons have the smallest receptive fields and receive the shortest-latency input from the receptor periphery. The S1 cortical area is conceptualized in current state of the art [16,17] as containing a single map of the receptor periphery. The somatosensory cortical network has a modular functional architecture and connectivity, with highly specific connectivity patterns [16-19], binding functionally distinct neuronal subpopulations from other cortical areas into motor circuit modules at several hierarchical levels [17]. The functional modules display a hierarchy of interleaved circuits connecting via inter-neurons in the spinal cord, in visual sensory areas, and in motor cortex with feed-back loops, and bilateral communication with supraspinal centers [17,18]. The from-local-to-global functional organization (Figure 1) of the somatosensory neural circuits relates to precise connectivity patterns, and these patterns frequently correlate with specific behavioral functions or motor output. Current state of the art suggests that developmental specification, where neuronal subpopulations are specified in the process of a precisely timed neurogenesis [17,1], determines the self-organizing nature of this connectivity for motor control and, in particular, limb movement control. The functional plasticity of the somatosensory cortical network is revealed by neuroscience research on the human primate [19] showing that somatosensory representations of fingers left intact after amputation of others on the same hand become expanded in less than ten days after amputation, when compared with representations in the intact hand of the same patient, or to representations in either hand of controls. Such network expansion reflects the functional resiliency of the self-organized somatosensory system, which has evolved as a function of active constraints [20], and in harmony with other sensory systems such as the visual and auditory brain. Grip force profiles are a direct reflection of the complex low-level, cognitive, and behavioral synergies this evolution has produced. The anterior intraparietal area (AIP) of the somatosensory map in particular seems involved in the internal processing and control of precision grasping, regardless of the hand in use [14,15], indicating that central grip force representation in the brain is not lateralized despite observable differences between forces produced by the dominant and non-dominant hands.

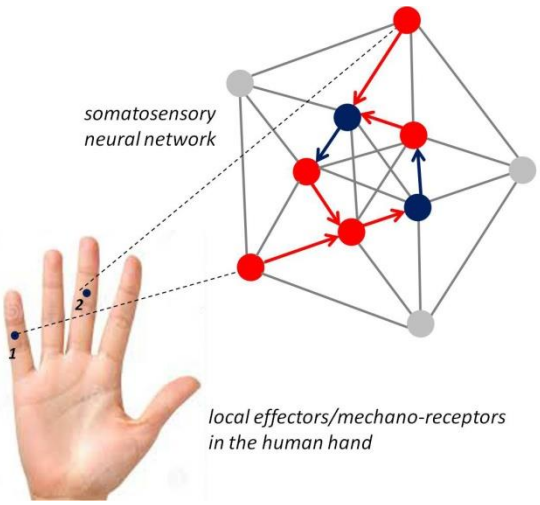

 doi:10.20944/preprints202010.0328.v1

Figure 1. Schematic representation of a fixed-size neural network in the somatosensory brain. Local effectors/mechanoreceptors on the middle phalanxes of the small (1) and the middle fingers (2) are indicated for illustration. Neural connectivity is arbitrarily chosen, and for illustration only; single nodes in the networks displayed graphically here may correspond to single neurons, or to a subpopulation of neurons with the same functional role. Red nodes may represent motor cortex (M) neurons, blue nodes may represent connecting visual neurons (V). Only one-way propagation is shown to keep the graphics simple, knowing that the somatosensory brain has multiple two-way propagation pathways with functional feed-back loops. It may be assumed that different levels of precision grip task expertise are reflected by different internal grip force representations in the neural networks of the somatosensory brain map, producing distinct observable variations in grip force coordination across fingers and hands.

Under the assumption that different levels of task expertise are inevitably reflected by different internal grip force representations in the neural networks of the somatosensory brain map, producing distinct observable variations in grip force coordination across fingers and hands, a functionally motivated step-by-step analysis is provided here. The analysis is aimed at highlighting specific observables of underlying differences in prehensile control strategies. In particular, it will be shown that the statistical correlation patterns between locally produced forces in the individual profiles deliver useful insight into how they may evolve with time and with training in a complex task where previously identified parameters affecting grip force in any single location may be difficult or impossible to control for. The example of multi-digit precision grip forces in a robot assisted task simulating minimally invasive surgery is exploited.

2. Materials and Methods

A wireless wearable (glove) sensor system was used here for collecting thousands of grip force data, per sensor location and individual user, in real time. The robotic system is designed for bi-manual intervention, and task simulations may solicit either the dominant or the non-dominant hand, as in our case here, or both hands at the same time, depending on the complexity of interventions. Here, four successive steps of a pick-and-drop task are simulated, requiring execution with either the dominant or the non-dominant hand through manipulation of the corresponding grip handle instrument of the system.

2.1 Slave Robotic System

The slave robotic system is built on the Anubis® platform of Karl Storz. This system consists of three flexible, cable-driven sub-systems describe in detail in our previous work [21,22] consisting of one main endoscope and two lateral flexible instruments. The endoscope carries the camera providing the visual feedback at its tip, and has two lateral channels which are deviated from the main direction by two flaps at the distal extremity. The instruments have bending extremities (one direction) and can be inserted inside the channels of the endoscope. This system has a tree-like architecture and the motions of the endoscope act also upon the position and orientation of the instruments. Two kinds of instruments are available: electrical instruments and mechanical instruments. Overall, the slave system has 10 motorized DoF. The main endoscope can be bent in two orthogonal directions. This allows moving the endoscopic view respectively from left to right and from up to down, as well as forward / backward. Each instrument has three DoF: translation (tz) and rotation (θz) in the endoscope channel, and deflection of the active extremity (angle β). The deflection is actuated by cables running through the instrument body from the proximal part up to the distal end. The mechanical instruments can be opened and closed.

2.2 Master/Slave Control

The slave robot is controlled at the joint level by a position loop running at 1000 Hz on a central controller. The master side consists of two specially designed interfaces, which are passive mobile mechanical systems. The user grasps two handles, each having 3 DoF, which translate for controlling instrument insertion, rotate around a horizontal axis for controlling instrument rotation,

Preprints (www.preprints.org) | NOT PEER-REVIEWED | Posted: 15 October 2020 doi:10.20944/preprints202010.0328.v1

and rotate around a final axis (moving with the previous DoF) for controlling instrument bending. These DoFs are similar to the possible motions of the instruments as demonstrated in preclinical trials [23]. Each handle is also equipped with a trigger and with a small four-way joystick for controlling camera movements. In the experiments here, the trigger is operated with the index finger of a given hand for controlling grasper opening and closing, the small joysticks for moving the endoscope are not used during task execution.

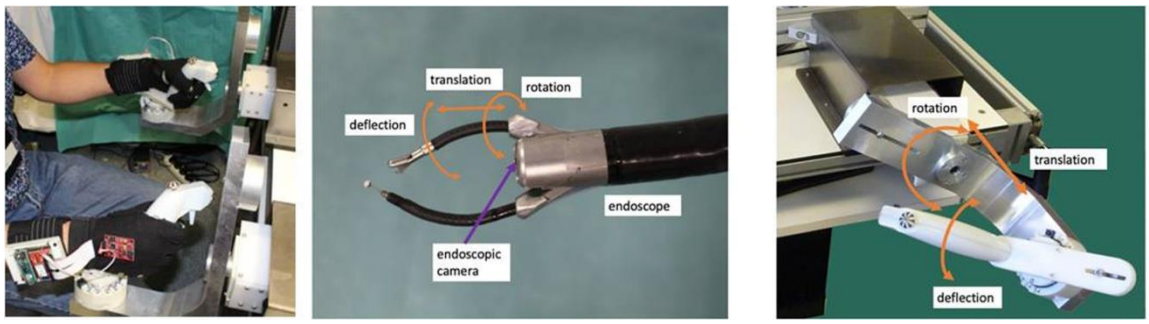

a) **b)**

Figure 2. Expert wearing the sensor gloves while manipulating the robotic master/slave system (**a**). Direction and type of tool-tip and control movements **(b).**

A high-level controller running on a computer under a real-time Linux OS communicates with the master interfaces and provides reference joint positions to the slave central controller. The user sits in front of the master console and looks at the endoscopic camera view displayed on the screen in front of him/her at a distance of about 80 cm while holding the two master handles, which are about 50 cm away from each other. Seat and screen heights are adjustable to optimal individual comfort. The two master interfaces are identical and the two slave instruments they control are also identical. Therefore, for a given task the same movements need to be produced by the user whatever the hand he/she uses (left or right). The master interfaces are statically balanced and all joints exhibit low friction, and therefore only minimal forces are required to produce movements in any direction. A snapshot view of a user wearing the sensor gloves while manipulating the handles of the system is shown in Figure 2a here above. The master-slave control chart of the master/slave system is displayed in Figure 2b. Figure 1c shows the different directions and types of tool-tip and control movements.

2.3 Sensor glove design

The system having its own grip style design, a specific wearable sensor system in terms of two gloves, one for each hand, with inbuilt Force Sensitive Resistors (FSR) was developed. The hardware and software configurations are described here below.

2.3.1 Hardware

The gloves designed for the study contain 12 FSR, in contact with specific locations on the inner surface of the hand as illustrated in Figure 3. Two layers of cloth were used and the FSR were inserted between the layers. The FSR did not interact, neither directly with the skin of the subject, nor with the master handles, which provided a comfortable feel when manipulating the system. FSR were sewn into the glove with a needle and thread. Each FSR was sewn to the cloth around the conducting surfaces (active areas). The electrical connections of the sensors were individually routed to the dorsal side of the hand and brought to a soft ribbon cable, connected to a small and very light electrical casing, strapped onto the upper part of the forearm and equipped with an Arduino microcontroller. Eight of the FSR, positioned in the palm of the hand and on the finger tips, had a 10 mm diameter, while the remaining four located on middle phalanxes had a 5mm

Preprints (www.preprints.org) | NOT PEER-REVIEWED | Posted: 15 October 2020 doi:10.20944/preprints202010.0328.v1

diameter. Each FSR was soldered to 10KΩ pull-down resistors to create a voltage divider, and the voltage read by the analog input of the Arduino is given by

$$V_{out} = R_{PD}V_{3.3}/(R_{PD}+R_{FSR}) \quad (1)$$

where R_{PD} is the resistance of the pull down resistor, R_{FSR} is the FSR resistance, and $V3.3$ is the 3.3 V supply voltage. FSR resistances can vary from 250Ω when subject to 20 Newton (N) to more than 10MΩ when no force is applied at all. The generated voltage varies monotonically between 0 and 3.22 Volt, as a function of the force applied, which is assumed uniform on the sensor surface. In the experiments here, forces applied did not exceed 10N, and voltages varied within the range of [0; 1500] mV. The relation between force and voltage is almost linear within this range. It was ensured that all sensors provided similar calibration curves. Thus, all following comparisons are directly between voltage levels at the millivolt (mV) scale. Regulated 3.3V was provided to the sensors from the Arduino. Power was provided by a 4.2V Li-Po battery enabling use of the glove system without any cable connections. The battery voltage level was controlled during the whole duration of the experiments by the Arduino and displayed continuously via the user interface. The glove system was connected to a computer for data storage via Bluetooth enabled wireless communication running at 115200 bits-per-second (bps).

Sensor	*Hand region*	*Anatomical reference*
S1	Thumb	Distal Phalanx
S2	Index	Distal Phalanx
S3	Middle	Distal Phalanx
S4	Index	Middle Phalanx
S5	Middle	Middle Phalanx
S6	Ring	Middle Phalanx
S7	Pinky	Middle Phalanx
S8	Palm	Head Metacarpal
S9	Palm	Head Metacarpal
S10	Palm	Shaft Metacarpal
S11	Palm	Base Metacarpal
S12	Palm	Base Metacarpal

Figure 3. Sensor locations on the inner surface of the dominant or non-dominant hand

2.3.2 Software

The software of the glove system was divided into two parts: one running on the gloves, and one for data collection. The general design of the glove system is described as follows. Each of the two gloves was sending data to the computer separately, and the software read the input values and stored them on the computer according to their header values indicating their origin. The software running on the Arduino was designed to acquire analog voltages provided by the FSR every 20 milliseconds (50Hz). In every loop, input voltages were merged with their time stamps and sensor identification. This data package was sent to the computer via Bluetooth, which was decoded by the computer software. The voltage data were saved in a text file for each sensor, with their time stamps and identifications. Furthermore, the computer software monitored the voltage values received from the gloves via a user interface showing the battery level. In case the battery level drops below 3.7 V, the system warns the user to change or charge the battery. However, this never occured during the experiments reported here.

 doi:10.20944/preprints202010.0328.v1

2.4 Experimental precision grip task

For this study, a *4-step pick-and-drop task* was designed. During the experiments, only one of the two instruments controlling the tool-tips (left or right, depending on the task session) was moved, while the main endoscope and its image remained still. The experiments started with the right or left hand gripper being pulled back. Then the user had to approach the object (*step 1*) with the distal tool extremity by manipulating the handles of the master system effectively. Then, the object had to be grasped with the tool (*step 2*). Once firmly held by the gripper, the object had to be moved to a position on top of the target box (*step 3*) with the distal extremity of the tool in the correct position for dropping the object into the target box without missing (*step 4*). To drop the object, the user had to open the gripper of the tool. The user started and ended a given task session by pushing a button, wirelessly connected to the computer. Grip force data were collected from one expert, who had been practicing with the system since its manufacturing and who is currently the most proficient user, familiar with using the system with his dominant and his non-dominant hand, one trained user who is reasonably familiar with using the system with his dominant hand, and one complete novice who had never used the system at all, and had no prior experience with any similar surgical system. The three users' hand sizes were about the same, and the sensor gloves were developed specifically to fit the hands of average-sized male individuals. The expert was left handed while the trained user and the novice were right handed. As explained earlier, the left and right interfaces are identical, and the same task is realized with either hand. Several thousands of grip force data were collected from the twelve sensor locations in the dominant and non-dominant hands of each of the three users in successive task sessions.

3. Results

A total of 459 348 grip force signals was recorded in the experiment, corresponding to a total of 38 279 grip force signals per sensor. For the expert user, we have a total of 4442 data per sensor from the dominant left hand recorded in real time across successive task sessions, and 6116 data per sensor from the non-dominant right hand. For the dominant-hand-trained user, we have a total of 5974 data from the dominant right hand, and 6760 data from the non-dominant left hand. For the total beginner (novice), we have 8484 data from the dominant right hand, and 6496 data from the non-dominant left hand. The full dataset is provided in Table S1 in the Supplementary section. Since a grip force signal from each sensor was acquired every 20 milliseconds in task time across sessions, a larger number of data from a given individual reflects longer task times. Here, we are dealing with a complex manual control task where different finger and hand locations are variably solicited during task execution, with significant differences as a function of task expertise, as shown in our previous work [21,22]. Thus, prior to any deeper statistical analysis, a descriptive evaluation needs to be performed to establish which of the twelve sensors produced task-relevant output data in terms of signals of at least 50 mV in at least 10% of the data.

3.1. Descriptive analyses

The column data from the spreadsheets were submitted to computation of the column means and the variance around the means in terms of standard errors. The results from these computations on the total number recorded for each sensor across users and hands are shown here below in Figure 4, followed by subsequent analysis for each sensor, user, and hand, shown further here below in Figure 5 (a,b,c). Analysis on the total number of data per sensor across users and hands (Figure 4) reveals that the sensor locations S1 and S4 on the distal phalanx of the thumb and the middle phalanx of the index were not sufficiently solicited during task execution to produce a signal in at least 10% of the total data recorded. As a consequence, S1 and S4 were eliminated from subsequent analyses. Further analyses on the total number of remaining sensors for each user and hand reveal insignificant activity levels in sensors 1, 2, 3, 4, 8 and 11 in the dominant hand of the expert (Figure 5 a, left), and in sensors 1, 3, 4 9 and 11 in the non-dominant hand (Figure 5a, right). The dominant hand of the trained user produced insignificant activity levels in sensors 1, 2, 3, 4, 7 and 11 (Figure

Preprints (www.preprints.org) | NOT PEER-REVIEWED | Posted: 15 October 2020 doi:10.20944/preprints202010.0328.v1

5b, left), and the non-dominant hand produced insignificant activity levels in sensors 1, 3, 4 5, 9, 11 and 12 (Figure 5b, right). In the novice data, insignificant activity levels in sensors 1 and 4 in the dominant hand (Figure 5c, left), and in sensors 1, 3, 4, 9 and 11 in the non-dominant hand (Figure 5c, right) were found.

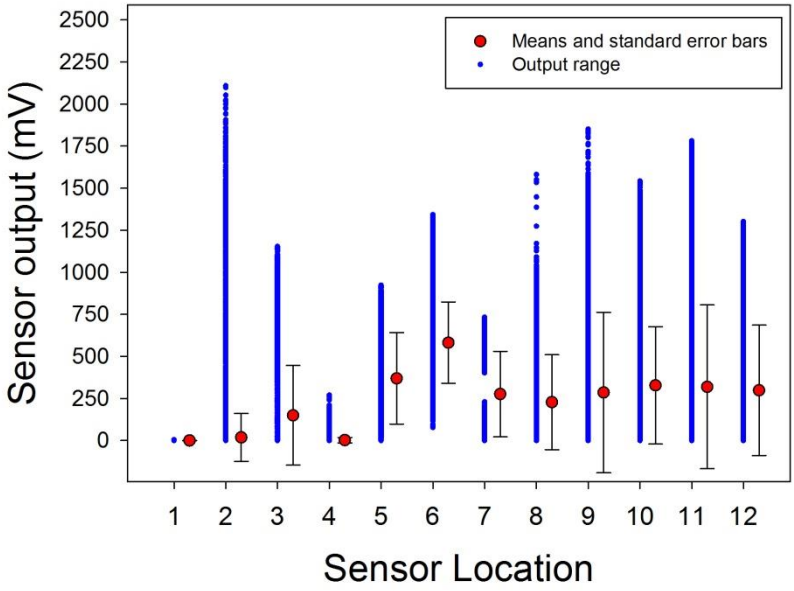

Figure 4. Means, standard errors, and output range between *minima* and *maxima* recorded from each of the twelve sensor locations across users and hands

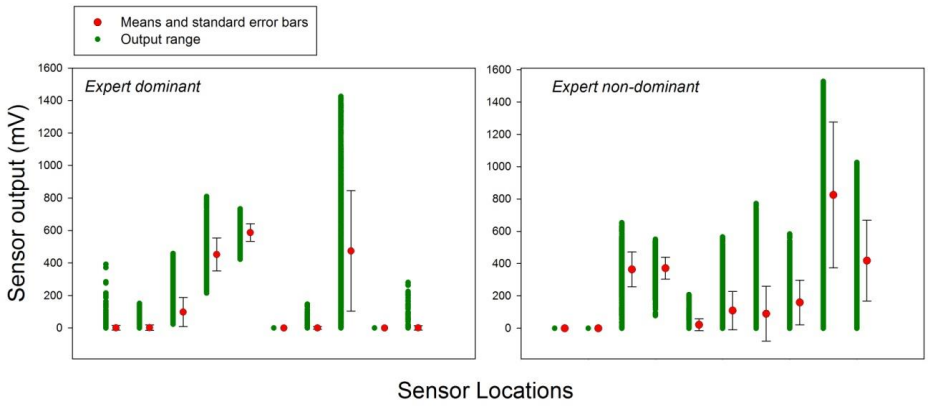

a)

Preprints (www.preprints.org) | NOT PEER-REVIEWED | Posted: 15 October 2020 doi:10.20944/preprints202010.0328.v1

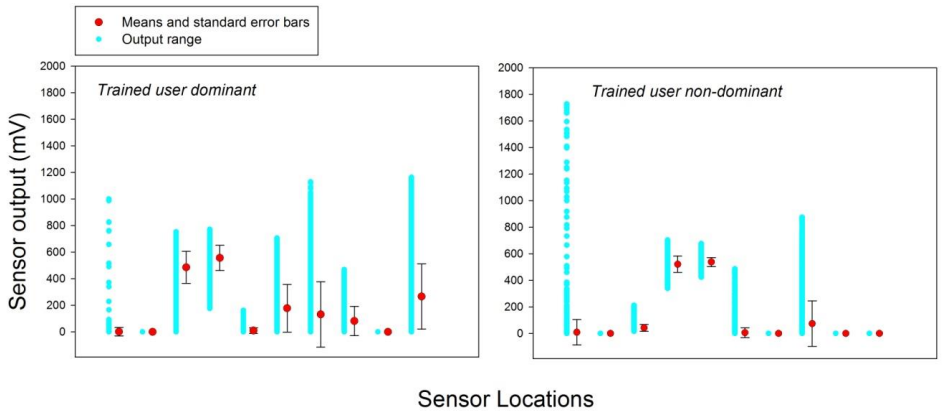

b)

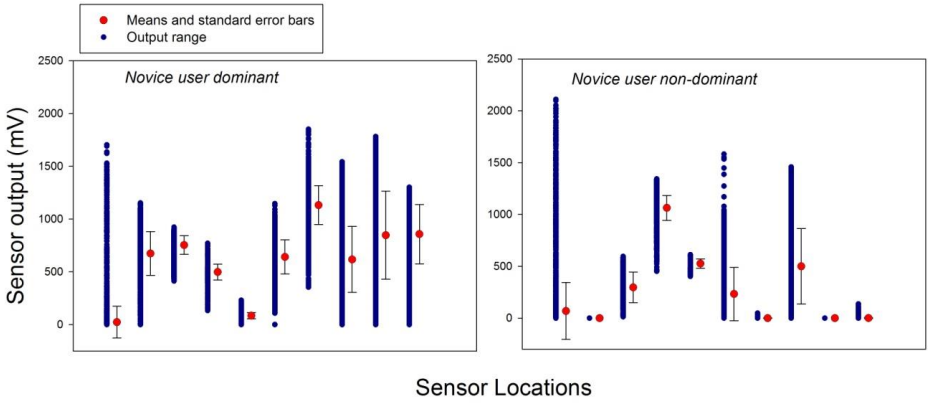

c)

Figure 5. Means, standard errors, and output range between *minima* and *maxima* recorded from sensor locations S2, S3, S5, S6, S7, S8, S9, S10, S11 and S12, from left to right on the x-axis of each graph, in the dominant and non-dominant hands of the expert user (a), the dominant-hand-trained user (b) and the novice (c).

Significant activity levels were recorded from sensor locations 5, 6, 7, 10 and 12 in the dominant hand of the expert (Figure 5 a, left), and in sensors 5, 6, 7, 8, 9, 10, 11 and 12 in the non-dominant hand (Figure 5a, right). The dominant hand of the trained user produced significant task-relevant activity levels in sensors 5, 6, 7, 8, 9, 10 and 12 (Figure 5b, left), and the non-dominant hand produced significant activity levels in sensors 2, 6, 7, 8 and 10 (Figure 5b, right). In the novice data, significant activity levels are found all sensors except 1 and 4 in the dominant hand (Figure 5c, left), and in sensors 5, 6, 7, 8, 10 and 12 in the non-dominant hand (Figure 5c, right). These descriptive analyses reveal, as a common characteristic to all users and hands, non-significant activation of sensors 1 and 4, and a considerable variation in significant task-relevant sensor activities between users and hands. As a consequence, a two-way analysis of variance (ANOVA) comparing between the three levels of the 'user' factor (expert, trained, novice) and the two levels of the 'hand' factor (dominant, non-dominant) to assess the statistical significance of between-factor variations for each sensor in which task-relevant activity was found in at least one user and hand, i.e. S2, S3, S5, S6, S7, S8, S9, S10, S11 and S12.

3.2. *Analysis of variance*

The two-way ANOVA, run separately for each of the active sensors as defined here above, returned statistically significant effects of the 'user' factor, the 'hand' factor and statistically

Preprints (www.preprints.org) | NOT PEER-REVIEWED | Posted: 15 October 2020 doi:10.20944/preprints202010.0328.v1

significant interaction between factors in each sensor, as revealed by the F values relative to these comparisons and their associated probability limits (P), shown here below in Table 1.

Table 1. Results from 2-way ANOVA on individual sensor data as a function of user and hand

General Linear Model

Source of Variation	**DF**	**SS**	**MS**	**F**	**P**
S2					
User	2	16773987,886	8386993,943	427,929	<0,001
Hand	1	2964227,230	2964 227,230	151,244	<0,001
User x Hand	2	3755368,124	1877684,062	95,805	<0,001
Residual	38271	750074008,984	19599,018		
Total	382763	57894773,041	87728,466		
S3					
User	2	1015096423,250	507548211,625	53513,867	<0,001
Hand	1	461998520,386	461998520,386	48711,289	<0,001
User x Hand	2	1021778383,168	510889191,584	53866,127	<0,001
Residual	38271	362978394,485	9484,424		
Total	382763	57894773,041	87728,466		
S5					
User	2	689902030,446	344951015,223	32517,606	<0,001
Hand	1	1395424378,812	1395424378,812	131542,911	<0,001
User x Hand	2	64882104,607	32441052,303	3058,131	<0,001
Residual	38271	405983767,489	10608,131		
Total	382762	8192985,527	73889,460		
S6					
User	2	894178539,095	447089269,547	58203,191	<0,001
Hand	1	380801423,473	380801423,473	49573,674	<0,001
User x Hand	2	695805856,940	347902928,470	45290,867	<0,001
Residual	38271	293979646,508	7681,525		
Total	382762	35427686,091	58402,855		
S7					
User	2	8131916,849	4065958,425	2996,062	<0,001
Hand	1	2415730452,996	2415730452,996	1780067,111	<0,001
User x Hand	2	25823790,450	12911895,225	9514,323	<0,001
Residual	38271	51937603,692	1357,101		
Total	382762	482530139,867	64858,662		
S8					
User	2	1182330765,802	591165382,901	24162,125	<0,001
Hand	1	488723290,475	488723290,475	19975,110	<0,001
User x Hand	2	162302567,526	81151283,763	3316,817	<0,001
Residual	38271	936361775,619	24466,614		
Total	382763	51959544,861	79735,593		
S9					

Preprints (www.preprints.org) | NOT PEER-REVIEWED | Posted: 15 October 2020 doi:10.20944/preprints202010.0328.v1

User	2	2331382489,784	1165691244,892	54035,820	<0,001
Hand	1	1875323478,829	1875323478,829	86930,946	<0,001
User x Hand	2	2332903972,891	1166451986,446	54071,085	<0,001
Residual	38271	825603632,161	21572,565		
Total	382768721314740,557		227853,348		
S10					
User	2	1576444413,907	788222206,954	11233,344	<0,001
Hand	1	36558031,549	36558031,549	521,007	<0,001
User x Hand	2	292642407,935	146321203,967	2085,296	<0,001
Residual	38271	2685402745,672	70168,084		
Total	382764653698608,118		121582,679		
S11					
User	2	1479234266,725	739617133,363	10404,163	<0,001
Hand	1	2866636795,456	2866636795,456	40324,860	<0,001
User x Hand	2	1479234266,725	739617133,363	10404,163	<0,001
Residual	38271	2720630817,886	71088,574		
Total	382769064486828,465		236819,073		
S12					
User	2	647731602,199	323865801,100	8786,483	<0,001
Hand	1	2434904432,621	2434904432,621	66058,985	<0,001
User x Hand	2	647217679,584	323608839,792	8779,511	<0,001
Residual	38271	1410651827,906	36859,550		
Total	38276	5733258645,998	149787,299		

The statistically significant two-way interactions are present in each of the sensors here and reflect the fact the users with different levels of training or task expertise use significantly different grip force control strategies, reflected by the variations in the recordings from their fingers and hands found here. The effect sizes underlying these significant variations between individuals and hands are reflected in terms of different means and standard errors, shown graphically here above in Figure 5 (a, b, and c). In order to gain insight into strategic differences reflected by the effects found here, co-variation *versus* independence of sensor activities was brought to the fore through correlation analyses (Pearson's product moment) performed on sensor data from each user and hand.

3.3. Correlation analyses

Pearson's product-moment correlation is expressed in terms of a coefficient ***r,*** shown in (1) here below, as a measure of the strength of a linear association between two variables indicating how far away all data points for x and y are from the line of best linear fit. The coefficient can take a range of values from +1 to -1. A value of zero indicates that there is no association between the two variables x and y. Values for ***r*** greater than zero indicates a positive correlation, values less than zero a negative correlation, where the value of one variable increases as the value of the other variable decreases. The product moment correlation expressed in terms of the coefficient (***r***) is calculated by dividing the covariance of two variables (x, y) by the product of their standard deviations. The form of the definition involves a product moment that is the mean or first moment of origin of the product of the mean-adjusted random variables:

$$(2) \quad \boldsymbol{r} = \mathrm{cov}(x,y)/(\mathrm{stddev}(x) \times \mathrm{stdev}(y))$$

Preprints (www.preprints.org) | NOT PEER-REVIEWED | Posted: 15 October 2020 doi:10.20944/preprints202010.0328.v1

Significant positive or negative correlations, in terms of ***r*** and the associated probability limits p, between sensor activities in each of the three users in their dominant and/or non-dominant hands are shown in Table 2 here below.

Table 2. Statistically significant correlations between sensor activities for each user

NOVICE USER dominant hand

	S5	S6	S7	S8	S9	S10	S11	S12
S3	.55			.57				
	p<.05			p<.05				
S5				.54	.48	.42	.60	
				p<.05	p<.05	p<.06	p<.01	
S6				.50	.65	.44		
				p<.05	p<.01	p<.05		
S7					.60	.47	.54	-.45
					p<.05	p<.05	p<.05	p<.05
S8					.55	.66	.36	
					p<.05	P<.01	p<.06	
S9						.46	.39	-.35
						p<.05	p<.06	p<.06
S10							.58	
							p<.01	
S11								-.46
								p<.05

TRAINED USER dominant hand

	S5	S6	S7	S8	S9	S10	S11	S12
S5				.46		.48		
				p<.05		p<.05		
S8						.67		
						p<.01		

EXPERT USER dominant (red highlights) and non-dominant (grey highlights) hands

	S5	S6	S7	S8	S9	S10	S11	S12
S5		.62				.53	.67	
		p<.001				p<.01	p<.001	
S6						.70	.55	
						p<.001	p<.001	
S8							.55	
							p<.01	

 doi:10.20944/preprints202010.0328.v1

S10	-.69 p<.01

The correlation analyses on grip force signals from the dominant right hand of the *novice user* (Table 2, top) reveal a total number of 18 positive and statistically significant correlations between sensor signals recorded from sensor 3 and signals from sensors 5 and 8, between signals recorded from 5 and signals from 8, 9, 10, and 11, between signals from sensor 6 and signals from 8, 9, and 10, between signals from sensor 7 and sensors 9, 10, and 11, between signals from sensor 8 and sensors 9, 10 and 11, between signals from sensor 9 and sensors 10 and 11, and between signals from sensor 10 and sensor 11. Statistically significant negative correlations were found between signals from sensors 7, 12, 9 and 11. No significant correlations were found between signals recorded from the non-dominant hand of the novice.

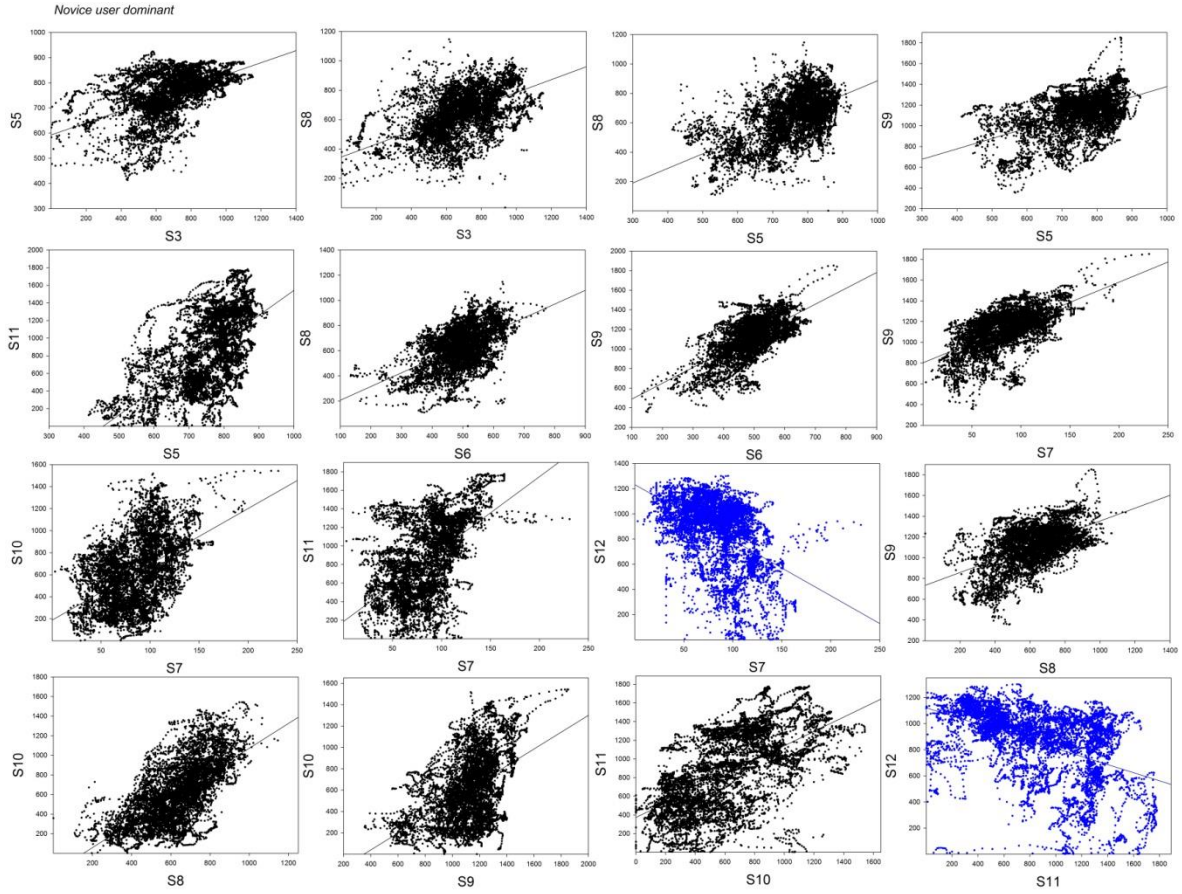

a)

Preprints (www.preprints.org) | NOT PEER-REVIEWED | Posted: 15 October 2020 doi:10.20944/preprints202010.0328.v1

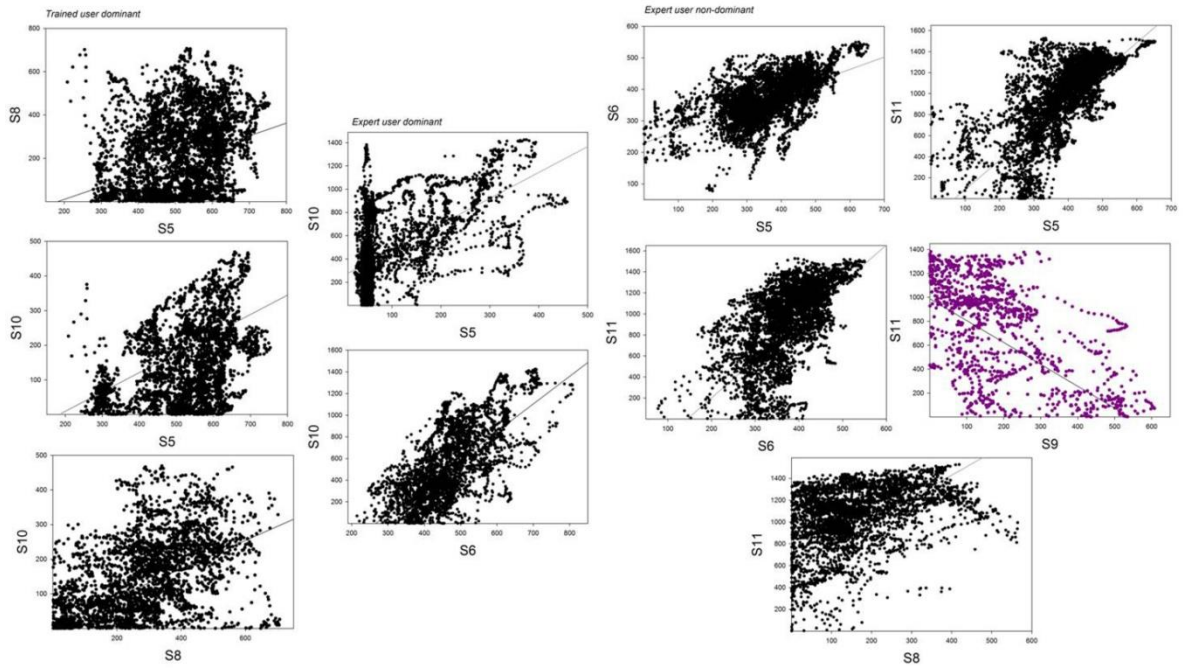

b) **c)**

Figure 6. Graphic representations of significant positive or negative sensor correlations (Pearson's product moment) between sensor signals in the dominant and/or non-dominant hands of the novice (a), the trained user (b), and the expert (c)

The correlation analyses on grip force signals from the dominant right hand of the *dominant-hand-trained user* (Table 2, middle) reveal a total number of 3 positive and statistically significant correlations between sensor signals recorded from sensor 5 and signals from sensors 8 and 10, and between signals from sensor 8 and signals from sensor 10. No significant correlations were found between signals recorded from the non-dominant hand of the dominant-hand trained user. The correlation analyses on grip force signals from the dominant left hand of the *expert user* (Table 2, bottom) reveal a total number of 2 positive and statistically significant correlations between sensor signals recorded from sensor 5 and signals recorded from sensor 10, and between signals recorded from sensor 6 and signals from sensor 10. In the non-dominant right hand, 4 statistically significant positive correlations were found between signals from sensor 5 and signals from sensors 6 and 11, between signals from sensor 6 and signals from sensor 11, and between signals from sensor 8 and signals from sensor 11. One statistically significant negative correlation was found between signals from sensor 10 and signals from sensor 11. Graphic representations of the sensor correlations are shown in Figure 6 a (novice user), b (trained user), and c (expert user). The correlation analyses reveal clearly that users with different levels of task training and expertise deploy employ different grip force strategies during the task for manual control of the robotic device handles. Based on prior knowledge relative to the putative roles of the different finger and hand regions reviewed in the introduction here above, a functional analysis of the sensor signal correlations found in the different hands of the three users is performed.

3.4. Functional analysis

Different grip force control strategies relating to difference in task expertise are reflected here by significant differences in grip forces in the different finger and hand locations reflecting different prehensile synergies at the central control levels in the neural networks of the somatotopically organized brain map in S1, as explained here above. While these central control levels are not directly observable in the grip force profiles, the correlations found here are the directly observable

Preprints (www.preprints.org) | NOT PEER-REVIEWED | Posted: 15 October 2020 doi:10.20944/preprints202010.0328.v1

consequence of these central differences. In subtle precision tasks, the fewer fingers are used, the greater is the grip control [4], and the largely redundant functional design of the human prehensile system [5] allows to achieve optimally parsimonious force deployment by as few fingers as necessary during task training through a variety of different strategies, as shown here below in Figure 7 in terms of strategy charts for grip force deployment in the dominant and non-dominant hands of the three users. From the functional charts in Figure 7 it becomes clear at a glance that the expert's dominant hand strategy is reflected by a parsimonious correlation between grip forces from hand and finger regions ensuring gross grip force deployment and control: the middle phalanxes of the ring and middle fingers and the base of the thumb. The same force correlation is found in the non-dominant hand of the expert, who is proficient with either hand in the task. As a consequence, the grip force strategy charts for the two hands are similar, with the exception that the non-dominant deploys additional force correlations with regions located in the palm of the hand. The strategy chart of the novice, in contrast, is characterized by a large number of functionally non-specific correlations between grip forces from almost all finger and hand regions of the dominant hand. These different levels of expertise of the three users here are reflected by other task parameters such as average session times and total number of incidents including number of drops, misses, and tool-trajectory adjustments. These are summarized further below in Table 3.

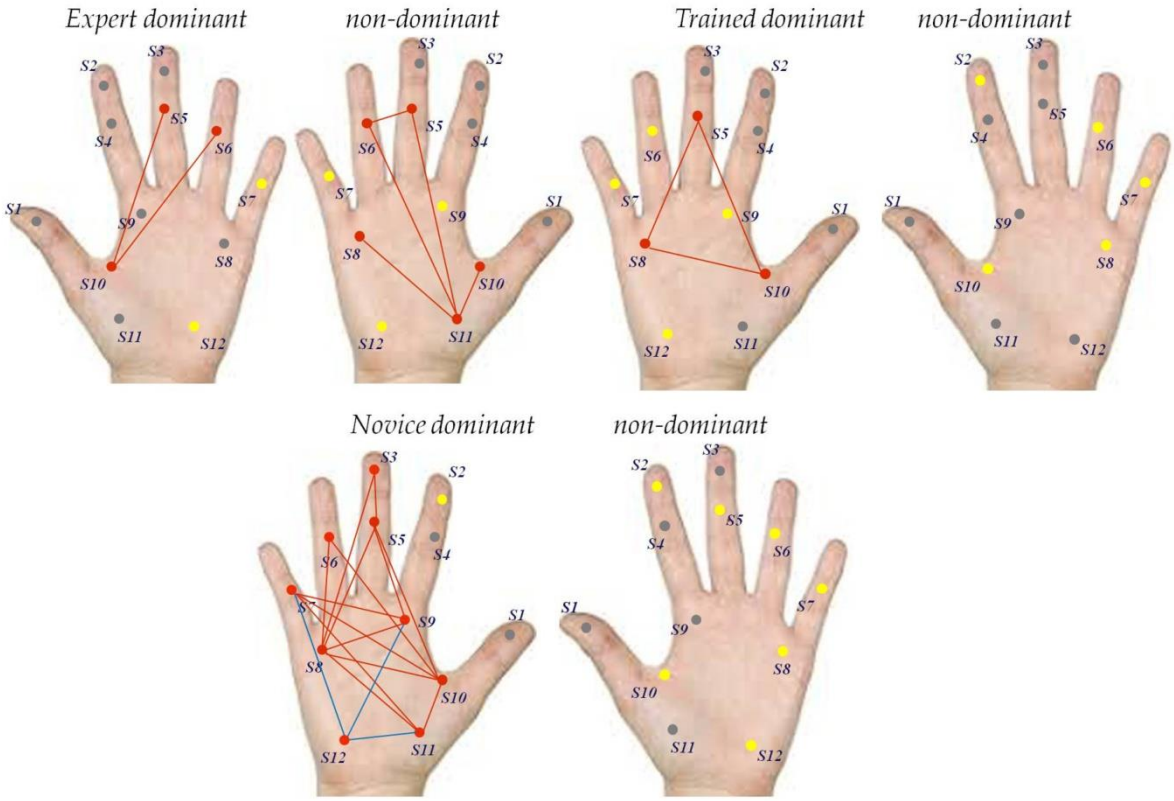

Figure 7. Functional strategy chart based on grip force signals and their positive/negative correlation, functional independence, or non-use in the precision grip task for the dominant and non-dominant hands of the expert (top left), the trained user (top right), and the expert (bottom). Non-activated grip force locations are highlighted as gray dots, independently active grip force locations as yellow, and significantly correlated locations as red dots. Red links between sensors indicate positive correlation, blue links indicate negative correlation.

Table 3. Average task completion time (seconds) and total number of incidents per user and hand used across task sessions

 doi:10.20944/preprints202010.0328.v1

	Time		Incidents	
	dominant	*non-dominant*	*dominant*	*non-dominant*
Novice	15.42	12.99	20	28
Trained	11.90	13.53	6	8
Expert	8.88	10.19	3	0

4. Discussion

Step-by-step statistics and correlation patterns for locally produced grip force signals in individuals with varying task proficiency deliver insight into how their grip force strategies evolve with time and training in complex tasks where single parameters affecting grip forces in the different regions of the hand used are difficult or impossible to control for. On the example of a multi-digit precision grip force robotic task, it is shown that different grip force control strategies relating to difference in task expertise are reflected by significant differences in grip forces in finger and hand locations which assume different roles for fine *versus* gross grip force control [4-10]. Individual grip force strategies and their evolution with training are governed by prehensile synergies at the central control levels in the neural networks of the somatotopically organized brain map in S1 [11-19]. While these central control levels are not directly observable in the grip force profiles, it can be assumed that different functional grip force strategy charts are the directly observable consequence of differences in their underlying brain representation. Patterns of covariation and/or independence of digit forces (prehensile synergies) depend on the task use history of each individual, which clarifies further why characteristics of individual digit action and interaction not only depend external constraints, but on a variety of other factors [2-5, 20-22]. One of the most challenging aspects of multivariate signal analysis in spatial and/or temporal domains is to be able to account for the functional structure/significance in the underlying signal(s). This has been achieved here by the correlation analyses to detect signal activities functionally linking neighboring sensory locations, highlighted by the individual grip force strategy charts from the functional analysis.

Grip force analysis on signals recorded in real time across multiple sensor regions in the fingers and the hand is a powerful means of tracking the evolution of an operator's or surgeon's individual force profile during task execution [21,22]. While current multi-modal feed-back systems may represent a slight advantage over the not very effective traditional single modality feedback solutions by achieving average grip forces closer to those normally possible with the human hand, the monitoring of individual grip forces of the surgeon (or trainee) during task execution by wearable multisensory systems is by far the superior solution. Real-time grip force sensing by wearable systems can directly help prevent incidents, because it includes the possibility of sending a signal (sound or light) to the operator or surgeon whenever his/her grip force exceeds a critical limit before the damage is done [24-29]. Proficiency, or expertise, in the control of a robotic master/slave system designed for minimally invasive surgery is reflected by a lesser grip force during task execution as well as by shorter task execution times [21,22,25,27]. Directly observable measures such as multi-digit grip forces recorded in real time, permit to define objective functional criteria for user expertise on precison systems such as robot-assisted surgical systems, which have a limited number degrees of freedom. Functional analyses like the one shown here are to be developed further to ensure the effective training of operators on highly complex manually controlled precision systems.

5. Conclusions

To read meaning into thousands of sensor data collected from multiple points of observation, functionally inspired descriptive and statistical "detective work" [2] is required before any further steps of automated data processing or modeling. This is illustrated here by a step-by-step approach towards deciphering observable correlations between thousands of grip force signals, recorded in real task time from multiple sensor locations, as the reflection of underlying central (brain) control mechanisms that evolve with training and hand use preferences.

Supplementary Materials: The following are available online at www.mdpi.com/xxx/s1: Table S1: original grip force data in microvolt.

Author Contributions: Conceptualization, B.D.L. and M.deM.; methodology, B.D.L., F.N. M.deM.; software, P.Z.; validation, F.N., P.Z. and B.D.L.; formal analysis, B.D.L.; investigation, F.N., B.D.L.; resources, P.Z.; data curation, F.N, B.D.L.; writing—original draft preparation, B.D.L.; writing—review and editing, B.D.L., F.N., M.deM.

Funding: This research received no external funding.

Acknowledgments: Material support from CNRS is gratefully acknowledged.

Conflicts of Interest: The authors declare no conflict of interest.

References

1. Di Rienzo M, Mukkamala R. Special Issue on Wearable and Nearable Biosensors and Systems for Healthcare. *Sensors (Basel)*, **2019**; https://www.mdpi.com/journal/sensors/special_issues/Nearable#
2. Tukey, J.W. Exploratory data analysis. *Methods* **1977**, *2*, 131–160, reprinted for sale in 2019.
3. H. Kinoshita, T. Murase, T. Bandou, Grip posture and forces during holding cylindrical objects with circular grips. *Ergonomics*, Vol. 39, Issue 9, 1996, pp. 1163-76.
4. H. Kinoshita, S. Kawai, K. Ikuta, Contributions and co-ordination of individual fingers in multiple finger prehension. *Ergonomics*, Vol. 38, Issue 6, 1995, pp. 1212-30.
5. ML. Latash, VM. Zatsiorsky. Multi-finger prehension: control of a redundant mechanical system. Adv Exp Med Biol, Vol. 629, 2009, pp. 597-618.
6. T. Oku T, S. Furuya, Skilful force control in expert pianists. *Exp Brain Res*, Vol. 235, Issue 5, 2017, pp. 1603-1615.
7. VM. Zatsiorsky, ML. Latash, Multifinger prehension: an overview. *J Mot Behav*, Vol. 40, Issue 5, 2008, pp. 446-76.
8. Y. Sun, J. Park, VM. Zatsiorsky, ML. Latash, Prehension synergies during smooth changes of the external torque. *Exp Brain Res*, Vol. 213, Issue4, 2011, pp. 493-506.
9. YH. Wu, VM. Zatsiorsky, ML. Latash, Static prehension of a horizontally oriented object in three dimensions. *Exp Brain Res*, Vol. 216, Issue 2, 202, 249-61.
10. SM. Cha, HD. Shin, KC Kim, JW. Park, Comparison of grip strength among 6 grip methods. *J Hand Surg Am*, Vol. 39, Issue 11, 2014, pp. 2277-84.
11. A. Cai, I. Pingel, D. Lorz, JP. Beier, RE. Horch, A. Arkudas, Force distribution of a cylindrical grip differs between dominant and nondominant hand in healthy subjects. *Arch Orthop Trauma Surg*, Vol. 138, Issue 9, 2018, pp. 1323-1331.
12. Buenaventura Castillo C, Lynch AG, Paracchini S. Different laterality indexes are poorly correlated with one another but consistently show the tendency of males and females to be more left- and right-lateralized, respectively. *R Soc Open Sci*. **2020**;*7*(4):191700.
13. Parsons LM, Gabrieli JD, Phelps EA, Gazzaniga MS. Cerebrally lateralized mental representations of hand shape and movement. J Neurosci. **1998**;18(16):6539-6548.
14. Davare M, Andres M, Clerget E, Thonnard JL, Olivier E. Temporal dissociation between hand shaping and grip force scaling in the anterior intraparietal area. *J Neurosci*. 2007;27(15):3974-3980.
15. Wilson S, Moore C. S1 somatotopic maps. Scholarpedia, **2015**; 10(4):8574.
16. Braun, C et al. Dynamic organization of the somatosensory cortex induced by motor activity. *Brain*, **2001**;124(11): 2259-2267.

17. Arber S. Motor circuits in action: specification, connectivity, and function. *Neuron*. **2012**;74(6):975-89.
18. Tripodi M, Arber S. Regulation of motor circuit assembly by spatial and temporal mechanisms. *Curr Opin Neurobiol*, **2012** ;22(4):615-23.
19. Weiss T et al. Rapid functional plasticity of the somatosensory cortex after finger amputation. *Experimental Brain Research,* **2000**;134(2): 199-203.
20. Young, RW Evolution of the human hand: The role of throwing and clubbing. *J Anat,* **2003**; 202:165–174.
21. Batmaz, AU, Falek, AM Zorn, L, Nageotte, F, Zanne, P, de Mathelin, M, Dresp-Langley, B. Novice and expert behavior while using a robot controlled surgery system In Proceedings of the 2017 13th IASTED International Conference on Biomedical Engineering (BioMed), Innsbruck, Austria, 21 February **2017**; pp. 94–99.
22. de Mathelin M, Nageotte F, Zanne P, Dresp-Langley B. Sensors for Expert Grip Force Profiling: Towards Benchmarking Manual Control of a Robotic Device for Surgical Tool Movements. *Sensors (Basel)*, **2019**;19(20).
23. Zorn, L, Nageotte, F, Zanne, P, Legner, A, Dallemagne, B, Marescaux, J, de Mathelin, M. A novel telemanipulated robotic assistant for surgical endoscopy: Preclinical application to ESD. *IEEE Trans. Biomed. Eng.* **2018**;*65*, 797–808.
24. González, A.G.; Rodríguez, D.R.; Sanz-Calcedo, J.G. Ergonomic analysis of the dimension of a precision tool handle: A case study. *Procedia Manuf,* **2017**; 13:1336–1343.
25. Batmaz, A.U.; de Mathelin, M.; Dresp-Langley, B. Seeing virtual while acting real: Visual display and strategy effects on the time and precision of eye-hand coordination. *PLoS ONE,* **2017**; 12:e0183789.
26. Dresp-Langley, B. Principles of perceptual grouping: Implications for image-guided surgery. *Front Psychol,* **2015**; 6:1565.
27. Dresp-Langley, B. Towards Expert-Based Speed–Precision Control in Early Simulator Training for Novice Surgeons. *Information*, **2018**; 9(12):316.
28. Dresp-Langley B, Monfouga M. Combining Visual Contrast Information with Sound Can Produce Faster Decisions. *Information*, 2019; 10(11):346-346.
29. Karageorghis CI, Cheek P, Simpson SD, Bigliassi M. Interactive effects of music tempi and intensities on grip strength and subjective affect. *Scand J Med Sci Sports*, **2018**; 28(3):1166-1175.

References must be numbered in order of appearance in the text (including citations in tables and legends) and listed individually at the end of the manuscript. We recommend preparing the references with a bibliography software package, such as EndNote, ReferenceManager or Zotero to avoid typing mistakes and duplicated references. Include the digital object identifier (DOI) for all references where available.